JOURNAL OF VIROLOGY, May 1996, p. 2697–2705 Vol. 70, No. 5
0022-538X/96/$04.00+0

Identification and Characterization of a Filament-Associated Protein Encoded by *Amsacta moorei* Entomopoxvirus

MOULAY HICHAM ALAOUI-ISMAILI[1,2] AND CHRISTOPHER D. RICHARDSON[1,2,3]*

Department of Microbiology and Immunology, McGill University, Montreal, Quebec, Canada H3A 2B4[1]; Amgen Institute and Ontario Cancer Institute, Toronto, Ontario, Canada M5G 2C1[2]; and Virology Group, Biotechnology Research Institute, National Research Council of Canada, Montreal, Quebec, Canada H4P 2R2[3]

Received 23 August 1995/Accepted 16 January 1996

A novel protein which is expressed at high levels in insect cells infected with *Amsacta moorei* entomopoxvirus was identified by our laboratory. This viral gene product migrates as a 25/27-kDa doublet when subjected to electrophoresis on sodium dodecyl sulfate-polyacrylamide gels. It is expressed at late times of infection and is present in infected cells but is absent in purified extracellular virions and occlusion bodies. The gene encoding this polypeptide was mapped on the viral genome, and cDNA clones were generated and sequenced. The predicted protein was shown to be phosphorylated and contained an unusual 10-unit proline-glutamic acid repeat element. A polyclonal antiserum was produced against a recombinant form of the protein expressed in *Escherichia coli*, and a monoclonal antibody which reacted with the proline-glutamic acid motif was also identified. Immunofluorescence and immunoelectron microscopy techniques revealed that this protein is associated with large cytoplasmic fibrils which accumulate in the cytoplasm between 96 and 120 h postinfection. We subsequently called this viral polypeptide filament-associated late protein of entomopoxvirus. The fibrils containing this polypeptide are closely associated with occlusion bodies and may play a role in their morphogenesis and maturation.

Entomopoxviruses (EPVs) are insect viruses which replicate in the cytoplasm of the host cell (2–4). Through structural and genetic similarities to the vertebrate poxviruses, as well as their cytoplasmic site of replication, these viruses were originally assigned to the family *Poxviridae* (33). The genomes of EPVs are composed of double-stranded linear DNA molecules ranging from 130 to 300 kb and characteristically have low G+C content (4, 34). The *Amsacta moorei* EPV (AmEPV) is the most studied member of this family of viruses, since several cell lines support its replication in vitro (12, 15, 30). AmEPV normally infects the larvae of the Indian red army worm (*A. moorei*) and the saltmarsh caterpillar (*Estigmene acrea*) (16, 25). Late in infection, this insect pathogen produces large oval-shaped structures called occlusion bodies or spheroids which accumulate in the cytoplasm of the infected cell (16). These structures are similar to the polyhedra produced in baculovirus infections (1, 3, 4, 13). Within these spheroids, the occluded virions are protected from environmental stress for extended periods of time, and these structures are important for the horizontal (insect-to-insect) transmission of the virus. On the other hand, the nonoccluded form of the virus is required for the spread of infection throughout the larvae (cell-to-cell transmission). Occlusion body formation is believed to begin around 72 h postinfection and involves the deposition of proteins around two or more mature virions (30). The AmEPV occlusion bodies are composed primarily of a cysteine-rich protein called spheroidin, which has a molecular mass of 110 kDa (5, 19, 26). The gene encoding this protein is under the control of a very strong promoter. As a result, spheroidin can constitute up to 40% of the total AmEPV-infected cell protein. However, when early viral protein synthesis or DNA replication is inhibited, the infected insect cells are unable to produce spheroids (31). On the other hand, nonoccluded EPV virions are still produced if the spheroidin gene is deleted (38). Unlike some other EPVs, AmEPV does not produce oval-shaped spindle bodies which are composed of fusolin protein (8, 10, 13). However, ultrastructural studies performed on AmEPV-infected insect cells (13, 31) and larvae (14) have shown the presence of large filamentous structures called cytoplasmic fibrils. It has recently been suggested that these fibrils may correspond to rearranged cellular cytoskeletal proteins. On the basis of phalloidin staining, actin has been reported to be associated with these structures (31), but biochemical and immunochemical evidence to support this hypothesis is lacking. By analogy, AcNPV (*Autographa californica* nuclear polyhedrosis virus) infections produce large bundles of filaments made up, at least in part, of a virally encoded protein called p10 (47, 52, 55). This protein may play a role in biogenesis of the polyhedron envelope.

We have identified a novel AmEPV protein which is expressed at high levels late in infection and migrates as a polypeptide doublet of 25 and 27 kDa when subjected to sodium dodecyl sulfate (SDS)-polyacrylamide gel electrophoresis (PAGE). This protein was called FALPE (filament-associated late protein of EPV). The gene encoding FALPE was mapped on the viral genome, and cDNA clones were identified and sequenced. We have also amplified, cloned, and sequenced the 5′ end of the FALPE transcript. A polyclonal antiserum was raised against FALPE expressed in bacteria and was used to immunoprecipitate both nonphosphorylated and ^{32}P-labeled forms of this protein. Finally, immunoelectron microscopy as well as immunofluorescence studies revealed that this protein is associated with the large cytoplasmic fibrils found in infected

* Corresponding author. Mailing address: Amgen Institute and Ontario Cancer Institute, 620 University Ave., Suite 706, Toronto, Ontario, Canada M5G 2C1. Phone: (416) 204-2280. Fax: (416) 204-2278. Electronic mail address: crichard@amgen.com.

cells. We propose that these fibrils may play a role in viral and/or occlusion body morphogenesis.

MATERIALS AND METHODS

Virus, cells, larvae, and viral genomic DNA. AmEPV was originally propagated in *E. acrea* larvae and later adapted to cell lines IPLB-LD-652 and BTI-EAA as described previously (5, 12). BTI-EAA cells and AmEPV originated from the laboratory of R. R. Granados (Boyce Thompson Institute for Plant Research, Ithaca, N.Y.). *Spodoptera frugiperda* (Sf9) cells were obtained from Max Summers (Texas A&M University), and they also supported the growth of AmEPV following several passages of adaptation. BTI-EAA and Sf9 cells were propagated in Grace's insect medium (GIBCO/BRL) supplemented with 10% fetal calf serum. The IPLB-LD-652 cells were cultivated in EX-CELL 400 serum-free medium (JRH Biosciences, Lenexa, Kans.). Amphotericin B (Fungizone; 2.5 μg/ml) and gentamicin (50 μg/ml) were added to prevent microbial contamination. AmEPV DNA was prepared from extracellular virus released from infected IPLB-LD-652 cells as previously described (5, 17).

Electrophoretic purification and amino-terminal sequencing of AmEPV FALPE. BTI-EAA cells were infected with nonoccluded virus at a multiplicity of infection of 1 to 5 PFU per cell. At 6 days postinfection, the cells were harvested and lysed with electrophoresis sample buffer containing 5% (vol/vol) β-mercaptoethanol and subjected to electrophoresis on 12% polyacrylamide gels in the presence of SDS (5). The gels were subsequently stained with Coomassie blue; protein bands corresponding to 25 and 27 kDa were excised and electroeluted in an Elutrap apparatus (Schleicher & Schuell). Eluted protein was dialyzed against phosphate-buffered saline (PBS), and each protein was again resolved by SDS-PAGE transferred to a polyvinylidene difluoride membrane (Millipore), and sequenced as previously described (5, 32), using an Applied Biosystems 470A gas-phase sequencer.

Degenerate oligonucleotides and specific DNA probes. A degenerate oligonucleotide (AmA_1), which spanned the coding region from amino acids 3 to 9 on the FALPE protein sequence, was synthesized. The AmA_1 sequence was 5′-GCICTICATCCAGTNAA(A/G)GA(T/C)(T/C)C-3′, where N represents any nucleotide and I represents the non-hydrogen-bounding nucleotide base inosine. AmAE and M13RE are analogous to AmA_1 and M13R (M13 reverse universal primer), respectively, except that they contained an additional *Eco*RI site plus two nucleotides at their 5′ termini.

Purified AmEPV DNA was digested with *Eco*RI. The resulting DNA fragments were ligated overnight to an *Eco*RI-cut plasmid pUC19, using bacteriophage T4 DNA ligase. The ligation mix was then used as a template for PCR in which either M13 or M13R, together with AmA_1, was used as a primer. The amplified DNA fragment obtained when M13R was used was called probe 1. This fragment was labeled with ^{32}P by using a Quick Prime kit (Pharmacia) and employed in subsequent experiments.

Construction of the AmEPV cDNA library and identification of FALPE cDNA clones. An AmEPV cDNA library was constructed in the bacterial cloning vector pUC19, using purified mRNA from infected IPLB-LD cells as previously described (5). This library was screened in two steps: (i) clones containing cDNAs specific for AmEPV were identified by probing this library with a ^{32}P-labeled *Hin*dIII-*Eco*RI restriction digest of viral genomic DNA; (ii) positive clones were then transferred to nylon membranes (Amersham) for the identification of FALPE clones. We generated a DNA probe for FALPE by digesting probe 1 with *Eco*RI. The resulting fragments were resolved on a 1.5% agarose gel, and a 288-nucleotide fragment free of pUC19 sequences was gel purified by using a Gene Clean kit (Bio 101, Inc.). This fragment was then radiolabeled as previously described (5) to yield probe 2 and hybridized to nylon membranes displaying the AmEPV cDNA. FALPE-specific clones were identified following autoradiography. DNA was sequenced, and Southern blot hybridizations to AmEPV genomic DNA were performed as previously described (5, 29).

Primer extension and analysis of the 5′ end of the FALPE transcript. A total of 1.5×10^8 Sf9 cells were infected with AmEPV. Four days postinfection, cells were harvested and poly(A)$^+$ mRNA was purified by using a Quickprep mRNA purification kit (Pharmacia). Subsequent experiments to determine the sequence of the 5′ end of the FALPE mRNA were performed by using the GIBCO/BRL 5′ RACE (rapid amplification of cDNA ends) system. An internal gene-specific primer, GSP1 (5′-CCAAGATTCTACTAGTTCAT-3′), was synthesized and used to reverse transcribe the 5′ end of FALPE mRNA. The 3′ end of the cDNA was dC tailed by using terminal deoxynucleotide transferase. A nested primer called GSP2 (5′-TGCTTCTTGTAAATAAC-3′) and an anchor primer which annealed to the dC tail at the 3′ end of cDNA were used to amplify a region corresponding to the 5′ end of the FALPE mRNA. The amplified DNA fragment was subsequently ligated to *Srf*I-cut pCR-Script SK(+) plasmid, cloned, and sequenced.

Expression of recombinant FALPE in *Escherichia coli*. Two oligonucleotides, $AmGB_2$ and $AmGL_2$, corresponding to the 5′ and 3′ ends, respectively, of the FALPE cDNA, were generated. $AmGB_2$ (5′-CGGGATCCTATAAAGAAACG TATTAGGGTTA-3′) contains a *Bam*HI site in addition to two extra nucleotides at its 5′ terminus, whereas $AmGL_2$ (5′-TTATTAGGTTCCGAATTGTGTGC AAGATTTTTAATTA-3′) has six additional nucleotides upstream of a *Hin*dIII site located at its 5′ end. These oligonucleotides were used as primers in a PCR to amplify the cDNA fragment that they flank. Once amplified, this fragment was cut with both *Bam*HI and *Hin*dIII and then inserted between these two sites in the bacterial expression plasmid PEZZ-18, supplied by Pharmacia (36, 37). The plasmid was introduced into *E. coli* DH5α cells by electroporation. Expression resulted in the production of a protein which accumulated inside the cell as inclusion bodies.

Antibodies. To prepare antigen for immunization, inclusion bodies containing the FALPE fusion protein were purified from transformed *E. coli* cells as previously described (27). Inclusion bodies were solubilized in 5 M guanidine-HCl and renatured by dialysis against Tris-HCl buffer (pH 8.0) containing 1 mM dithiothreitol protease inhibitors, and 20% glycerol. The solubilized recombinant protein was then purified through an immunoglobulin G (IgG) column containing a 2-ml bed volume of IgG-Sepharose 6 Fast Flow (Pharmacia) and eluted with buffer containing 1 M NaCl. The purified protein was subsequently injected into a rabbit for the production of a polyclonal antibody (pAbFALPE) (20). Anti-*Trypanosoma brucei brucei* procyclin monoclonal antibody (MAb) CLP001, which recognizes the proline-glutamic acid (PE) repeat portion of the FALPE protein (42), was purchased from Cedarlane Laboratories Ltd. (Mississauga, Ontario, Canada). For subsequent immunoblot analysis, AmEPV-infected insect cells were resuspended in sample buffer, and the proteins were resolved by SDS-PAGE, transferred onto nitrocellulose membranes, and probed with either the polyclonal or monoclonal antibody. Antibody-antigen complexes were detected with alkaline phosphatase-conjugated donkey anti-rabbit or anti-mouse IgG antibodies (Jackson Immunoresearch Laboratories) as previously described (20, 51). Fluorescein-conjugated donkey anti-mouse antibody used in fluorescence microscopy studies was purchased from Cedarlane Laboratories. Donkey anti-rabbit IgG or goat anti-mouse IgG conjugated to 12-nm gold particles was obtained from Jackson Immunoresearch and used in immunoelectron microscopy studies.

Labeling AmEPV-infected cells with $^{32}P_i$ and immunoprecipitation of FALPE. A total of 1.5×10^6 BTI-EAA cells were infected with AmEPV. Four days postinfection, the medium was removed and replaced with phosphate-free Grace's medium (45, 51). Following 3 h of incubation in phosphate-free medium, $^{32}P_i$ (ICN) was added at a concentration of 1 mCi/ml, and the cells were incubated for a further 6 h. Radiolabeled cellular proteins were solubilized in 1 ml of radioimmunoprecipitation assay (RIPA) buffer (150 mM NaCl, 1% [vol/vol] Nonidet P-40, 0.5% [wt/vol] sodium deoxycholate, 0.1% [wt/vol] SDS, 50 mM Tris-HCl [pH 7.5]) containing 0.1% (wt/vol) bovine serum albumin (BSA) and protease inhibitors. Immunoprecipitations were performed on 200 μl of this cell lysate as previously described (51). Precipitated proteins were resuspended in sample buffer and resolved by SDS-PAGE. The gels were finally exposed to Kodak XAR-5 X-ray film.

Incubation of FALPE with CIP. A total of 7.5×10^3 mock-infected or AmEPV-infected Sf9 cells were harvested 6 days postinfection and lysed in 500 ml of RIPA buffer. One half of this cell lysate was dialyzed on a floating 0.025-μm-pore-size VSWP membrane (Millipore) against calf intestinal alkaline phosphatase (CIP) buffer (41). The other half was equilibrated against CIP buffer containing 10 mM Na_2HPO_4, which is a phosphatase inhibitor. Samples were incubated with 3.4 U of CIP (Pharmacia) and subsequently analyzed by SDS-PAGE and by immunoblotting as previously described (51).

Immunoelectron microscopy. AmEPV-infected Sf9 or IPLB-LD-652 cells were harvested 4, 5, and 6 days postinfection and fixed with 1% (wt/vol) paraformaldehyde and 1% (vol/vol) glutaraldehyde in PBS. Cells were infiltrated with LR White, polymerized, cut into thin sections, and placed onto nickel grids. Cell sections were preincubated with 1% (wt/vol) BSA and subsequently with either MAb CLP001 or pAbFALPE at a dilution of 1:800 or 1:1,000, respectively. Sections were washed in PBS containing 0.05% Tween 20 and incubated for 30 min with a 1:20 dilution of either donkey anti-rabbit IgG or goat anti-mouse IgG conjugated to 12-nm gold particles. Finally, grids were washed with PBS containing 0.05% Tween 20 and then with water and stained for 5 min with uranyl acetate and 2 min with lead citrate prior to visualization with a Philips EM400 microscope.

Immunofluorescence and confocal microscopy. Sf9 or BTI-EAA cells were infected with AmEPV at a multiplicity of infection of 10 PFU/ml. Cells were harvested 5 days postinfection, washed by centrifugation at $400 \times g$, and resuspended in PBS at 10^6 cells per ml. For viewing through a conventional fluorescence microscope, cells were attached to microscope slides by centrifugation at $10{,}000 \times g$ for 7 min in a Cytospin centrifuge (20). Alternatively, prior to observation through a confocal microscope, cells were plated on microscope slides pretreated with poly-L-lysine (Sigma Biosciences) and were allowed to attach for 20 min (20). Slides were subsequently immersed in 0.25% glutaraldehyde solution in PBS for 20 min, washed twice in PBS, and then permeabilized and fixed with cold methanol-acetone (1:1) for 20 min. The fixed cells were incubated with MAb CLP001 at a dilution 1:1,000 in Grace's medium (containing 10% fetal calf serum) for 30 min and then washed three times in PBS. Identical results were obtained if cells were fixed with 2% paraformaldehyde in PBS followed by cold methanol-acetone (1:1) or just simply cold methanol-acetone (1:1). The bound antibody was visualized by using fluorescein-conjugated goat anti-mouse antibody at a 1:25 dilution in culture medium. To visualize actin, fixed and permeabilized cells were incubated with phalloidin conjugated to rhodamine (Sigma) at a concentration of 0.2 μg/ml. Fluorescent structures were visualized with either a Leitz fluorescence microscope or a Molecular Dynamics Multiprobe 2001 confocal microscope.

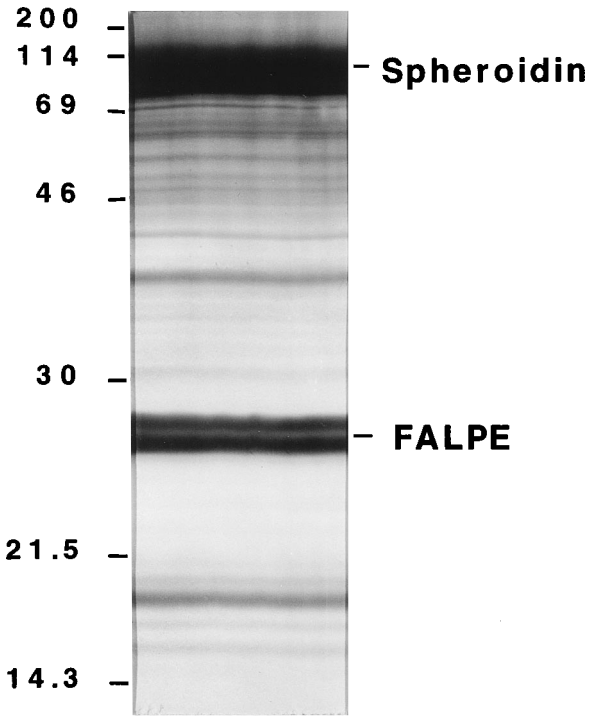

FIG. 1. Infected cell proteins resolved by SDS-PAGE and stained with Coomassie blue. Total protein extracts from BTI-EAA cells infected with AmEPV were prepared at 6 days postinfection. Proteins were solubilized in sample buffer containing SDS and β-mercaptoethanol and resolved on an SDS–12% polyacrylamide gel. Proteins were subsequently stained with Coomassie blue. Migration of molecular weight standards (in kilodaltons) is indicated at the left. The major occlusion body protein, spheroidin, migrates with a molecular mass of 110 kDa. In addition, a major 25/27-kDa protein doublet was evident and was subsequently called FALPE.

Nucleotide sequence accession number. The nucleotide sequence of FALPE was submitted to GenBank and has the accession number U30297.

RESULTS

AmEPV major late proteins and purification of FALPE. BTI-EAA cells infected with AmEPV were harvested 7 days postinfection and solubilized in sample buffer containing 5% (vol/vol) β-mercaptoethanol, and proteins were resolved by SDS-PAGE and stained with Coomassie blue (Fig. 1). The most predominant protein, migrating at about 110 kDa, corresponds to the major occlusion body protein, spheroidin (5, 19, 26). Two other major bands were detected and migrated with apparent molecular masses of 25 and 27 kDa. These were gel purified and subjected to amino-terminal sequencing. The same 29-amino-acid sequence, AP(P)VDPVKDLIKKTI?VIA NIDQSTKKIL, was obtained for both bands, suggesting that this doublet corresponds to two modified species of the same protein. This gene product was synthesized as a 25/27-kDa protein made late in infection and was subsequently designated FALPE.

Mapping the location of the gene for FALPE on the AmEPV genome. A degenerate oligonucleotide, AmA_1, was designed and synthesized from amino acid residues 6 to 9 of the amino-terminal protein sequence of FALPE. AmA_1, in combination with either M13 or M13R, was used as a primer in PCRs in order to amplify a portion of the gene encoding FALPE which had been cloned into the bacterial plasmid pUC18. *Eco*RI-digested AmEPV DNA was ligated to the *Eco*RI site of pUC18 and used as template for this reaction. This strategy produced a 308-nucleotide DNA fragment when M13R was used. A second round of PCR amplification was then performed with AmAE and M13R. AmAE is a homolog to AmA_1 but contains an *Eco*RI site at its 5′ terminus. The resulting fragment was subsequently digested with *Eco*RI and cloned at the *Eco*RI site of pUC18, and the DNA was sequenced. Analysis of the deduced amino acid sequence from this DNA revealed that the first 22 amino acids coded for by one of the fragment's ends were identical to residues 6 to 28 of the N-terminal protein sequence of FALPE, which had been determined by Edman degradation. This finding indicated that the 308-nucleotide DNA fragment represented a portion of the FALPE gene; we called the fragment probe 1 and used it in subsequent experiments.

AmEPV DNA was purified as described in Materials and Methods and digested with either *Eco*RI, *Hin*dIII, *Acc*I, or *Eco*RV. The resulting fragments were resolved on an agarose gel, transferred onto a nitrocellulose membrane, and subsequently hybridized to ^{32}P-labeled probe 1. As shown in Fig. 2, hybrid-

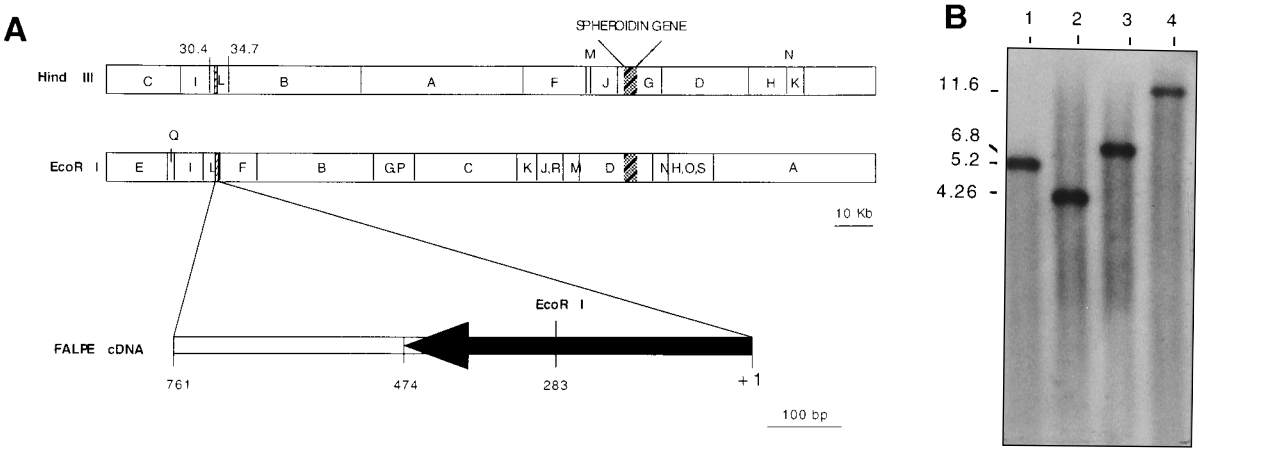

FIG. 2. Localization of the gene for FALPE on the AmEPV genome by Southern blot hybridization. (A) FALPE is encoded by an ORF (shown as a black arrow) located in the *Hin*dIII L and *Eco*RI L restriction fragments and a small portion of the *Eco*RI F restriction fragment. The position of the spheroidin gene is also indicated. (B) Southern blot hybridization of AmEPV genomic DNA digested with *Acc*I (lane 1), *Hin*dIII (lane 2), *Eco*RV (lane 3), and *Eco*RI (lane 4). Restriction fragments were resolved on a 0.7% agarose gel, transferred to a nitrocellulose membrane, and hybridized to probe 1, which is specific for the FALPE gene. The blot was exposed to X-ray film. Sizes (in kilodaltons) of standard DNA fragments are shown at the left.

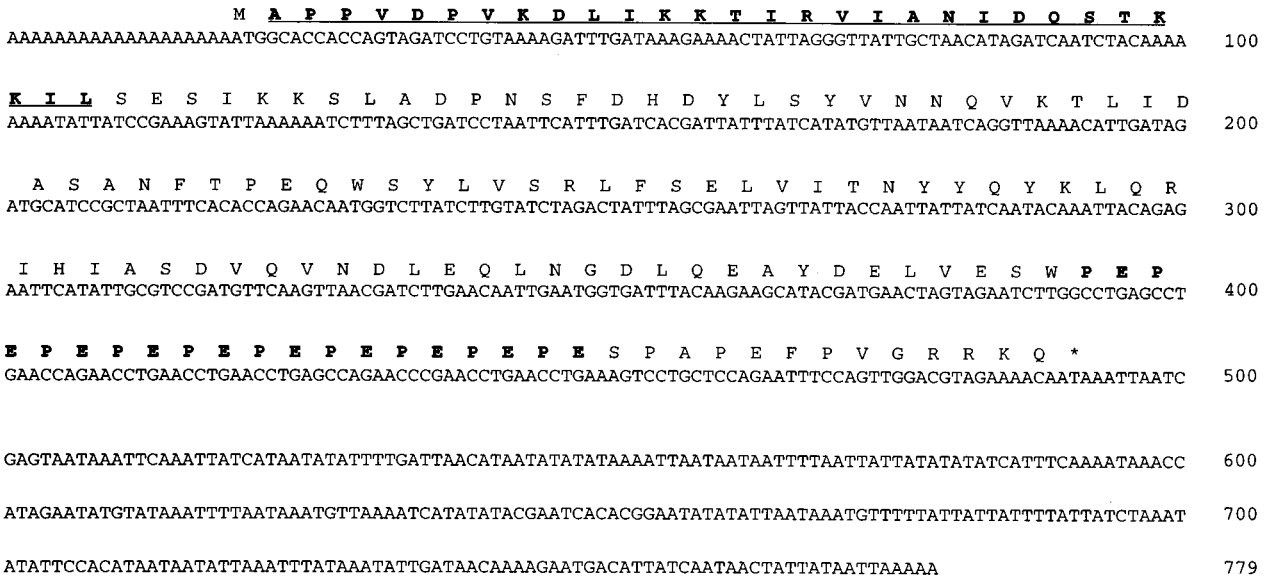

FIG. 3. Predicted amino acid sequence of FALPE and cDNA nucleotide sequence derived from its mRNA. A 759-nucleotide cDNA fragment found in pLP17 was sequenced, and the 5′ end of the FALPE mRNA was deduced by RACE as described in Materials and Methods. Amino acids which were determined directly by N-terminal sequencing of 25/27-kDa polypeptides eluted from SDS-polyacrylamide gels are underlined. The unusual PE repeat motif is in boldface.

ization occurred with an 11.6-kb *Eco*RI fragment (*Eco*RI-F) and to the 4.26-kb *Hin*dIII fragment (*Hin*dIII-L), as determined from a genomic map which had previously been reported (18). In addition, probe 1 hybridized to both 5.2-kb *Acc*I and 6.8-kb *Bgl*II fragments. These results suggest that FALPE is encoded by an AmEPV gene and that this gene is present as a single copy within the viral genome.

Identification and sequencing of FALPE cDNA clones. The 308 bp of probe 1 contained 20 bp at the 3′ end of the FALPE coding region which were derived from the multicloning site of pUC18 following PCR with the M13R primer. To facilitate further screening of pUC19 constructs, probe 2 was generated to remove these 20 bp after *Eco*RI digestion as described in Materials and Methods. Probe 2 was gel purified, ^{32}P labeled, and used to probe an AmEPV cDNA library cloned into pUC19. Eight related clones hybridized to probe 2 and were sequenced. Clone pLP17 was found to contain most of the coding sequence for FALPE (Fig. 3). The cDNA fragment found in pLP17 is 759 nucleotides long; the 5′-most codon found in the predicted open reading frame (ORF) corresponds to the sixth amino acid (proline) found in the protein sequence of FALPE which had been determined by N-terminal sequencing of the protein. The predicted 17.3-kDa protein encoded by the ORF contains 10 tandem repeats of a two-amino-acid (PE) motif at its carboxy terminus (Fig. 3). We suspect that this region causes retardation of the protein's migration through SDS-polyacrylamide gels, resulting in the 25/27-kDa doublet observed on our gels. The significance of this tandem amino acid repeat was investigated by a computer-assisted homology search which identified a few proteins containing similar domains. The most striking homolog to FALPE is procyclin, which is the major glycoprotein found on the surface of *T. brucei brucei* during its procyclic phase. This protein contains 15 repeats of the same PE motif (42). The early E1A proteins of adenovirus types 2 and 5 (11, 50) also contain six repeats of the PE motif. To our knowledge, no distinct role has been assigned to these regions in E1A protein or procyclin. This region may be important for protein structure, or it could function in protein-protein interaction (56). The FALPE cDNA contains an *Eco*RI site one-third of the way from its 5′ terminus; the 3′ end of the FALPE ORF is contained in the *Eco*RI L fragment of the AmEPV genome, while the 5′ third is situated in the *Eco*RI F fragment (Fig. 2B).

Amplification and cloning of the 5′ end of FALPE cDNA. Total mRNA was purified from AmEPV-infected Sf9 cells at 4 days postinfection. An oligonucleotide complementary to the FALPE cDNA sequence beginning at position 354 downstream from the first codon in pLP17, called GSP1, was annealed to this mRNA and used as a primer to generate a cDNA by reverse transcription. This DNA was dC tailed and then amplified by PCR using a nested primer, GSP2, together with an anchor primer specific for the 5′ tail. We obtained a fragment 430 bp long which was subsequently cloned in the pCR-Script SK(+) plasmid and then sequenced as described in Materials and Methods. In addition to identifying the nucleotide sequence which corresponds the six first amino acids of the protein, analysis of the 430-bp fragment revealed two interesting features of the 5′ end of the FALPE transcript: (i) the presence of a poly(A) tract about 20 nucleotides long at its 5′ end and (ii) the absence of any other untranslated sequences between this poly(A) region and the translation initiation signal ATG. These features are characteristic of poxvirus late transcripts (3, 5, 9, 19, 35). This result not only indicates that this protein is encoded by the AmEPV genome but further suggests that FALPE is a typical poxvirus late protein and its transcription is regulated through recognized poxvirus motifs.

Temporal expression of FALPE in infected cells. To confirm that this protein is expressed late in infection, Sf9 cells were infected with AmEPV and harvested at different times postinfection. Proteins were separated by SDS-PAGE and transferred to a nitrocellulose membrane. The blot was subsequently probed with MAb CLP001 in order to monitor the accumulation of FALPE. Typical results obtained for this cell line are shown in Fig. 4; the more slowly migrating 27-kDa species was detected at 72 h postinfection, while the 25-kDa species appeared 24 h later. Both polypeptides accumulated in the infected cells up to 120 h postinfection. A time course analysis of BTI-EAA cells infected with AmEPV yielded similar results (data not shown). Previous observations demonstrated that nonoccluded virus was typically released between 72 and 120 h

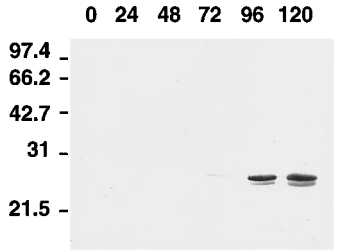

FIG. 4. Time course analysis of FALPE synthesized in infected insect cells. Sf9 cells inoculated with AmEPV were harvested at 0, 24, 48, 72, 96, and 120 h postinfection. Total cell proteins were solubilized in sample buffer, subjected to electrophoresis on a 12% polyacrylamide gel, and transferred onto a nitrocellulose membrane. MAb CLP001 was used to detect FALPE. Sizes (in kilodaltons) are indicated on the left.

postinfection and that the early thymidine kinase protein and viral DNA were synthesized between 12 and 24 h postinfection (17, 25, 29). Occlusion bodies in the cytoplasm first became evident between 72 and 120 h postinfection (5, 30). Thus, the pattern of expression of FALPE indicates that this protein is expressed at late times during AmEPV infections. This observation agrees with our previous results concerning the nature of the 5′ terminus of the FALPE mRNA transcript, which is typical of late gene expression by poxviruses (9).

Bacterial expression of FALPE. The cDNA fragment within pLP17 was amplified by PCR and subcloned between the *Bam*HI and *Hin*dIII sites of the bacterial expression vector PEZZ-18. Expression from this plasmid resulted in the production of a FALPE-protein A fusion protein with a combined molecular mass of 45 kDa, as determined by its migration through SDS-polyacrylamide gels. The expressed polypeptide product accumulated within *E. coli* as inclusion bodies. Immunoblot analysis showed that this fusion protein was specifically recognized by MAb CLP001, indicating that the fusion product indeed contained FALPE (data not shown). The bacterial inclusion bodies were isolated and solubilized, and the recombinant protein was purified through an IgG column as described in Materials and Methods. The fusion protein was then injected into a rabbit for the production of the polyclonal antiserum pAbFALPE.

FALPE is a phosphorylated protein. Computer analysis of the predicted amino acid sequence of FALPE revealed the presence of four potential protein kinase C phosphorylation sites (located at amino acid residues 15, 25, 26, and 33) in addition to three potential casein kinase phosphorylation sites (located at amino acid residues 37, 58, and 123). To determine whether this protein was actually phosphorylated, AmEPV-infected Sf9 cells were labeled with ^{32}P at 4 days postinfection. Infected cell proteins were immunoprecipitated with pAbFALPE and resolved by SDS-PAGE. Preimmune antiserum was used as a control for nonspecific immunoprecipitation. Following autoradiography of the gels, a single protein migrating at about 25 kDa was detected exclusively in the pAbFALPE immunoprecipitate, suggesting that the protein is phosphorylated (Fig. 5A). To confirm this result, proteins from AmEPV-infected Sf9 cells were resuspended in RIPA buffer 6 days postinfection and treated with CIP in the presence or the absence of the phosphatase inhibitor Na_2HPO_4. The samples were resolved by SDS-PAGE, and FALPE was detected by immunoblot analysis using MAb CLP001 (Fig. 5B). Only the 27-kDa species was revealed by this antibody after phosphatase treatment (lane 2). However, when the incubation was performed in the presence of Na_2HPO_4 (lane 1) or if CIP was omitted (lane 3), both the 25- and 27-kDa species, as well as some faster-migrating minor species, were evident on the immunoblot. Similar results were obtained with BTI-EAA and IPLB-LD cells infected with AmEPV. These data support the conclusion that FALPE is phosphorylated and that phosphorylation resulted in faster migration of the protein through SDS-polyacrylamide gels. A number of sites appear to be phosphorylated, as evidenced by the multiple bands shown in lanes 1 and 3 of Fig. 5B. The faster mobility of phosphorylated FALPE on SDS-gels may be due to an increase in negative charge on the protein. It was interesting that a total extract from *E. acrea* larvae infected with AmEPV contained the phosphorylated form of FALPE almost exclusively; treatment of this protein with CIP also converted it to the 27-kDa dephosphorylated species (data not shown).

Localization of FALPE by immunoelectron microscopy and morphogenesis of occlusion bodies in AmEPV-infected-Sf9 cells. Sf9 cells were infected with AmEPV and harvested at 4 and 6 days postinfection. In the following experiments, FALPE was localized by immunogold electron microscopy using either pAbFALPE or MAb CLP001. Many of the features characteristic of poxvirus infections were evident (12, 30). Electron-dense type I viroplasms, in which DNA replication and the first stages of virus assembly occur, were evident early in infection. Crescent membrane structures were present, and virions associated with multilaminar membranes were observed in the cytoplasm in structures known as type II viroplasms. At 96 h postinfection, cytoplasmic bundles of filaments were observed close to assembling virions. The bundles possessed a wool-like appearance, ranged from 1 to 5 μm in length, and often contained 50 or more separate filaments. Each individual filament was estimated to be between 10 and 15 nm in diameter. Typical cytoplasmic filament bundles are shown in Fig. 6A; these structures did not react with preimmune serum. However, the fibrils did react with either the pAbFALPE or MAb CLP001.

Immunogold labeling of cytoplasmic filaments with polyclonal antisera directed against FALPE is shown in Fig. 6B. These cytoplasmic fibrils have been reported previously by a number of investigators (12, 14, 16, 22, 30, 31) and are believed to be characteristic of EPV infections. At later times of infection, these bundles become more frequent in number and the diameters of the fibrils containing aggregated filaments are larger. These bundles often appear to be in close association with the periphery of the occlusion bodies (Fig. 6C and 6D). In

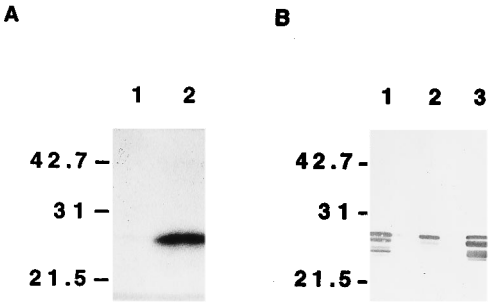

FIG. 5. Demonstration that FALPE is a phosphoprotein through metabolic labeling and studies with CIP. (A) BTI-EAA cells were infected with AmEPV and labeled with $^{32}P_i$ at 96 h postinfection as described in Materials and Methods. Cells were lysed in RIPA buffer, and proteins were immunoprecipitated with preimmune antiserum (lane 1) or pAbFALPE (lane 2) and subjected to electrophoresis on SDS-polyacrylamide gels. Labeled proteins were detected by exposing the gel to X-ray film. (B) Cell lysates from BTI-EAA cells infected with AmEPV were prepared at 144 h postinfection and treated with CIP in the presence (lane 1) or absence (lane 2) of phosphatase inhibitor (10 mM Na_2HPO_4). Untreated cell lysate is shown in lane 3. Proteins were subsequently resolved on an SDS–12% polyacrylamide gel and transferred to a nitrocellulose membrane. MAb CLP001 was then used to reveal FALPE. Sizes (in kilodaltons) are indicated on the left.

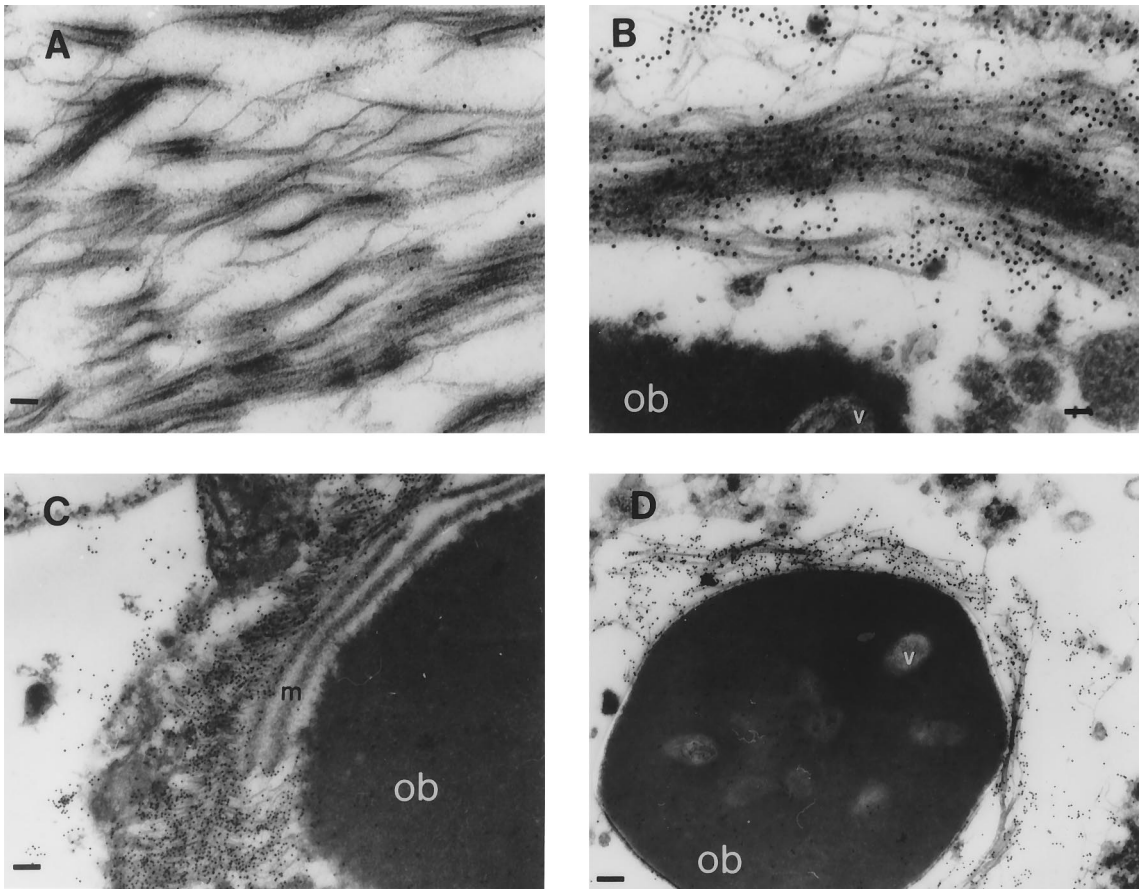

FIG. 6. Immunogold electron microscopy of Sf9 insect cells infected with AmEPV, using antibodies specific for FALPE. Cells were harvested at 144 h infection, fixed, and sectioned as described in Materials and Methods. Cell sections were incubated with preimmune rabbit polyclonal antibody (A), mouse MAb CLP001 (B and C), or rabbit polyclonal antibody pAbFALPE (D). Structures containing FALPE were revealed by using gold conjugated to either goat anti-rabbit or goat anti-mouse antibodies, and specimens were subsequently viewed through a Philips EM400 electron microscope. Bars: A, 0.10 μm; B, 0.13 μm; C, 0.20 μm; D, 0.24 μm. ob, v, and m represent occlusion body, virion, and membrane of occlusion body, respectively. Magnifications: A, ×92,300; B, ×75,900; C, ×47,000; D, ×40,940.

Sf9 cells, occlusion bodies are frequently surrounded by a multilayer envelope consisting of one to four layers of an electron-dense material (Fig. 6C). FALPE resides on the cytoplasmic side of these structures and is initially diffuse and spongy, but it condenses and compacts as the occlusion body matures. Cytoplasmic fibrils appear to surround the occlusion bodies (Fig. 6D). FALPE appears to be a key component of these cytoplasmic filaments and may play a role in AmEPV occlusion body morphogenesis.

Immunofluorescence microscopy of Sf9 cells infected with AmEPV, using FALPE antibodies. AmEPV-infected Sf9 cells were harvested at 96, 120, and 144 h postinfection, fixed with glutaraldehyde, and permeabilized as described in Materials and Methods. MAb CLP001 was then used to detect FALPE in the infected cells. Similar staining patterns were obtained with 2% paraformaldehyde followed by cold acetone-methanol fixation or simply by cold acetone-methanol treatment. Consistent with our observations by immunogold electron microscopy, we found that this protein was associated with long cytoplasmic filaments (Fig. 7A to D). However, the cytoplasmic fibrils was even more extensive than first shown by electron microscopy, and they formed a loose network surrounding the nucleus of the infected cell (Fig. 7A). The diameter and length of these fibrils increased between 96 to 120 h infection (Fig. 7B). Occlusion bodies are closely associated with these fibrils at 144 h postinfection (Fig. 7C). The number of occlusion bodies in the cell closely parallels the number of cytoplasmic fibrils present. Over the course of infection, the fibrils increased from 0.1 to 0.75 μm in diameter and were often 5 to 15 μm in length (Fig. 7D). Uninfected cells did not exhibit these fluorescent structures, nor was background staining significant (data not shown). In addition, treatment of infected cells at 48 h postinfection with either cytochalasin D (5 μg/ml) or colchicine (30 μg/ml) which disrupts microfilaments or microtubules, respectively, had no effect on the FALPE filament structures (data not shown).

A previous report hypothesized that the cytoplasmic fibers observed in cells infected with AmEPV might be due to rearrangements of F-actin (31). Virus infection was observed to produce a reorganization of the host cell cytoskeleton: a progressive disassembly of both the microtubule and filament network during the period of AmEPV infection was followed by polymerization of F-actin to yield small bundles or spikes which were associated with virus assembly. To probe this possibility, experiments were performed with phalloidin, a fungal metabolite which binds to F-actin. Rhodamine-conjugated phalloidin and MAb CLP001 were used to label Sf9 cells infected with AmEPV at 144 h postinfection. The FALPE-specific MAb was detected by incubating the cells with fluorescein-conjugated goat anti-mouse IgG. Fluorescently labeled cells were observed with a Molecular Dynamics Multiprobe 2001 confocal microscope. The results in Fig. 7E, which were obtained irrespective of the method of fixation, showed that the FALPE-associated cytoplasmic filaments (shown in green)

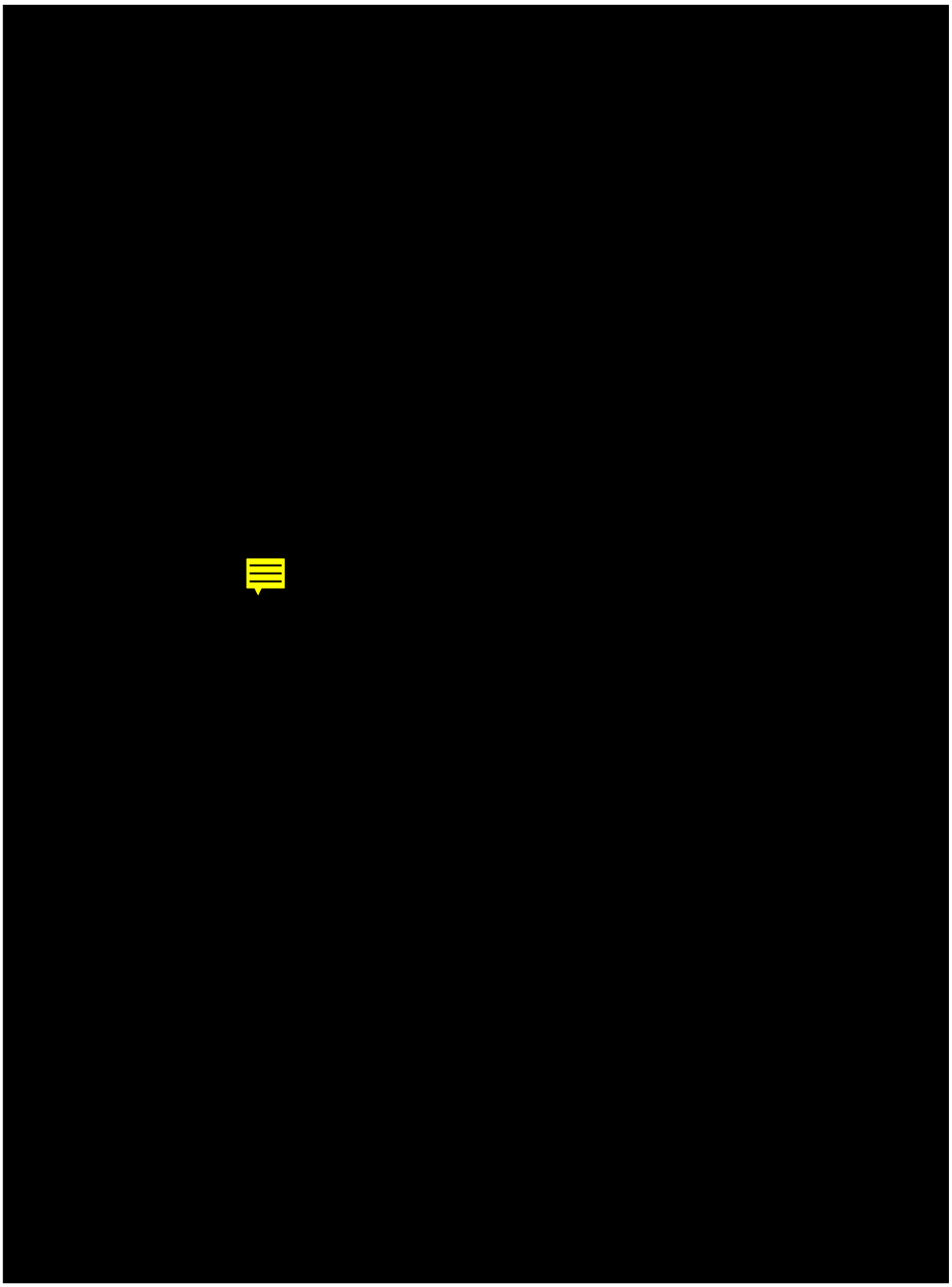

FIG. 7. Immunofluorescence and confocal microscopy of Sf9 cells infected with AmEPV, using antibodies specific for FALPE. Sf9 cells were inoculated with AmEPV and harvested at 96 h (A), 120 h (B), and 144 h (C to E) postinfection. Cells were fixed and stained with MAb CLP001, and fluorescent structures were visualized by using goat anti-mouse antibodies conjugated to fluorescein. Occlusion bodies were shown to associate with the fibrils (C). Some Sf9 cells were stained with, in addition to MAb CLP001, phalloidin conjugated to rhodamine, which binds to and reveals F-actin (E). Actin and FALPE staining were found to be distinct. Cells were viewed by conventional fluorescence microscopy (A to D) or confocal microscopy (E). Bars in panels A to D represent 4 μm; the bar in panel E indicates 5 μm.

were distinct from the F-actin network (shown in red) in the infected cell at this time of infection. Phalloidin appears to stain isolated patches or spikes of filaments rather than the long cables associated with FALPE. We also demonstrated that the cytoplasmic fibrils containing FALPE did not react with antibodies directed against the microtubule protein, tubulin (data not shown). Thus, the EPV protein FALPE appears to be associated with unique cytoplasmic structures which are produced at late times during AmEPV infections. The external surfaces of these filamentous structures appear to be devoid of actin and tubulin, but the possibility that additional viral and cellular components are associated with these fibrils remains to be determined.

DISCUSSION

A novel phosphoprotein which is associated with filamentous structures was discovered in insect cells infected with AmEPV and called FALPE. The protein migrates on SDS-polyacrylamide gels as a doublet consisting of polypeptides with molecular masses of 25 and 27 kDa. The amino acid sequence contains an unusual 10-unit PE repeat which appears to cause this viral late gene product to move more slowly than the predicted 17.5-kDa polypeptide. Experiments which involved labeling this protein with ^{32}P or treatment of the phosphoprotein with phosphatase indicated that the fast-migrating 25-kDa species was actually associated with phosphate groups. We hypothesize that multiple phosphorylation sites could increase the overall negative charge of the protein, causing it to move faster toward the anode during electrophoresis. The actual role of phosphorylation in the biological function of this protein is unclear. At any rate, FALPE is not present in purified virions or occlusion bodies. It does, however, form a network of cytoplasmic fibrils composed of 50 to 100 filaments which appear to be associated with AmEPV occlusion body assembly and maturation late in infection.

Only a few proteins other than FALPE contain the unusual PE repeat motif. These include the E1A protein, which is a transactivator of the adenovirus major late promoter (11, 50), the outer membrane procyclin protein of *T. brucei brucei* (42), a periplasmic iron transport protein from *E. coli* called TonB (40, 46), the ryanodine drug receptor on skeletal muscle cells (57), and a newly reported uncharacterized gene product specified by the *Eco*RI C fragment of AcNPV (23). Repeating short proline repeats are generally believed to play a role in protein-protein interaction (56). Proline residues contain flat structures which can accept electrons and interact with flat aromatic rings such as those belonging to phenylalanine. In addition, a PE repeat characteristically forms a polyproline type II helix structure (56) which may be important in the association of filaments and formation of bundles.

Virus replication and assembly have historically been reported to be associated with the cytoskeleton (28, 39). Vaccinia virus, a mammalian poxvirus, assembles in cytoplasmic factories associated with cytoplasmic fibers. High-voltage electron microscopy of infected cells revealed that membrane enclosed vaccinia virions aligned themselves with these structures (44). Immunofluorescence studies indicated that the fibers are actin-containing filaments of the cell cytoskeleton (21). Mature virions are drawn into specialized microvilli which contain filaments and are subsequently released into the medium. More recently, vaccinia virus was shown to encode a homolog of the cellular actin-binding protein, profilin (6). However, this protein was diffusely distributed throughout the cytoplasm and did not appear to associate with actin in the infected cells. This profilin homolog could also be deleted without affecting virus replication. Other viruses have been reported to synthesize filament-associated proteins. The E4 protein of human papillomaviruses has been shown to colocalize with cytokeratin intermediate filament networks (43) and may play a role in the collapse of the cellular cytoskeleton and pathogenesis of warts.

Baculoviruses are another group of insect viruses, but unlike EPVs, they replicate in the nuclei of their host cells. Cellular actin has been purported to play a role in AcNPV nucleocapsid morphogenesis in the nucleus (7, 53). However, another baculovirus protein, called p10 (24), has been shown to form filamentous structures which are associated with AcNPV occusion body structures at late times of infection (47, 52). The exact function of p10 is not known, but it may play a role in occlusion body envelope formation or nuclear lysis, which would favor dissemination of the virus (48, 49, 52, 55). The time of appearance and ultrastructure of the p10 structures are somewhat analogous to the situation with FALPE-associated filaments in cells infected with AmEPV. Both types of structures consist of bundles of filaments which are associated with occlusion bodies late in infection. These two proteins could conceivably play similar roles during infection.

Immunofluorescence and confocal microscopy indicated that actin-containing bundles and FALPE filament structures were distinct and separate. However, until the filaments are biochemically analyzed, we cannot totally rule out the possibility that phalloidin and antitubulin binding sites are masked by the abundant quantities of FALPE present in these structures. Actin could be stained with phalloidin or MAbs to yield small cytoplasmic patches, while antibodies specific for FALPE illuminated vast cytoplasmic networks devoid of actin. The extensive network of cytoplasmic fibrils composed of FALPE appear to be different from the more diffuse actin-containing structures found by Marlow et al. in studies using rhodamine-conjugated phalloidin (31). Electron microscopy and immunofluorescence demonstrated that the cytoplasmic bundles are synthesized late in infection and are tightly associated with occlusion bodies and maturing virions. Whether these structures are essential for AmEPV replication remains to be determined; we are currently trying to delete this gene through homologous recombination, as has been done previously with the p10 gene of baculoviruses (54) and the spheroidin gene of AmEPV (38). The quantity and density of cytoplasmic fibrils produced appear proportional to the number of occlusion bodies generated during AmEPV infections. This observation again suggests that occlusion body maturation is somehow related to the presence of these fibrils. Whether other viral or cellular proteins are also associated with the cytoplasmic fibrils is currently being investigated by isolating these structures through biochemical fractionation. In addition, immunofluorescence microscopy using antibodies directed against other known filament proteins is being performed.

ACKNOWLEDGMENTS

We thank Kathy Hewitt at the McGill University EM Centre for assistance with electron microscopy.

This work was funded by Medical Research Council of Canada operating grant MA10638. M.H.A.-I. was partially supported by an F. C. Harrison graduate student fellowship from McGill University and a Canadian International Development Agency scholarship.

REFERENCES

1. **Adams, J. R., and J. T. McClintock.** 1991. Baculoviridae. Nuclear polyhedrosis viruses. Part 1. Nuclear polyhedrosis viruses of insects, p. 187–204. *In* J. R. Adams and J. R. Bonami (ed.), Atlas of invertebrate viruses. CRC Press, Boca Raton, Fla.
2. **Arif, B. M.** 1984. The entomopoxviruses. Adv. Virus Res. **29:**195–213.
3. **Arif, B. M.** 1995. Recent advances in the molecular biology of entomopoxviruses. J. Gen. Virol. **76:**1–13.
4. **Arif, B. M., and E. Kurstak.** 1991. The entomopoxviruses, p. 179–195. *In* E.

Kurstak (ed.), Viruses of invertebrates. Marcel Dekker Publishers, New York.
5. **Banville, M., F. Dumas, S. Trifiro, B. Arif, and C. Richardson.** 1992. The predicted amino acid sequence of the spheroidin protein from *Amsacta moorei* entomopoxvirus: lack of homology between major occlusion body proteins of different poxviruses. J. Gen. Virol. **73:**559–566.
6. **Blasco, R., N. B. Cole, and B. Moss.** 1991. Sequence analysis, expression, and deletion of vaccinia virus gene encoding a homolog of profilin, a eukaryotic actin-binding protein. J. Virol. **65:**4598–4608.
7. **Charlton, C. A., and L. E. Volkman.** 1991. Sequential rearrangement and nuclear polymerization of actin in baculovirus-infected *Spodoptera frugiperda* cells. J. Virol. **65:**1219–1227.
8. **Dall, D., A. Sriskantha, A. Vera, J. Lai-Fook, and T. Symonds.** 1993. The gene encoding a highly expressed spindle body protein of *Heliothis armigera* entomopoxvirus. J. Gen. Virol. **74:**1811–1818.
9. **Dhavalkumar, D. P., and D. J. Pickup.** 1987. Messenger RNAs of a strongly-expressed late gene of cowpox virus contain 5′-terminal poly(A) sequences. EMBO J. **6:**3787–3794.
10. **Gauthier, L., F. Cousserans, J. C. Veyrunes, and M. Bergoin.** 1995. The *Melolontha melolontha* entomopoxvirus (MmEPV) fusolin is related to the fusolins of lepidopteran EPVs and to the 37K baculovirus glycoprotein. Virology **208:**427–436.
11. **Gingeras, T. R., D. Sciaky, R. E. Gelinas, J. Bing-Dong, C. E. Yen, M. M. Kelly, P. A. Bullock, B. L. Parsons, K. E. O'Neil, and R. J. Roberts.** 1982. Nucleotide sequences from the adenovirus-2 genome. J. Biol. Chem. **257:** 13475–13491.
12. **Goodwin, R. H., J. R. Adams, and M. Shapiro.** 1990. Replication of the entomopoxvirus from *Amsacta moorei* in serum-free cultures of a gypsy moth cell line. J. Invertebr. Pathol. **56:**190–205.
13. **Goodwin, R. H., R. J. Milner, and C. D. Beaton.** 1991. Entomopoxvirinae, p. 259–285. *In* J. R. Adams and J. R. Bonami (ed.), Atlas of invertebrate viruses. CRC Press, Boca Raton, Fla.
14. **Granados, R. R.** 1973. Insect poxviruses: pathology, morphology, and development. Misc. Publ. Entomol. Soc. Am. **9:**73–94.
15. **Granados, R. R.** 1981. Entomopoxvirus infections in insects, p. 102–126. *In* E. W. Davidson (ed.), Pathogenesis of invertebrate microbial disease. Allenheld Press, Totowa, N.J.
16. **Granados, R. R., and D. W. Roberts.** 1970. Electron microscopy of a poxlike virus infecting an invertebrate host. Virology **40:**230–243.
17. **Gruidl, M. E., R. L. Hall, and R. W. Moyer.** 1992. Mapping and molecular characterization of a functional thymidine kinase from *Amsacta moorei* entomopoxvirus. Virology **186:**507–516.
18. **Hall, R. L., and W. F. Hink.** 1989. Physical mapping and field inversion electrophoresis of *Amsacta moorei* entomopoxvirus DNA. Arch. Virol. **110:** 77–90.
19. **Hall, R. L., and R. M. Moyer.** 1991. Identification, cloning, and sequencing of a fragment of *Amsacta moorei* entomopoxvirus DNA containing the spheroidin gene and three vaccinia virus-related open reading frames. J. Virol. **65:**6516–6527.
20. **Harlow, E., and D. Lane.** 1988. Antibodies. A laboratory manual. Cold Spring Harbor Laboratory, Cold Spring Harbor, N.Y.
21. **Hiller, G., C. Jungwirth, and K. Weber.** 1981. Fluorescence microscopical analysis of the life cycle of vaccinia virus in chick embryo fibroblasts. Virus-cytoskeleton interactions. Exp. Cell Res. **132:**81–87.
22. **Hukuhara, T., J. Xu, and K. Yano.** 1990. Replication of an entomopoxvirus in two lepidopteran cell lines. J. Invertebr. Pathol. **56:**222–232.
23. **Kool, M., R. Broer, D. Zuidema, R. W. Golbach, and J. M. Vlak.** 1994. Nucleotide sequence and genetic organization of 7.3 kb region (map unit 47 to 52.5) of *Autographa californica* nuclear polyhedrosis virus fragment EcoR I-C. J. Gen. Virol. **75:**487–494.
24. **Kuzio, J., D. Z. Rohel, C. J. Curry, A. Krebs, E. B. Carstens, and P. Faulkner.** 1984. Nucleotide sequence of the p10 polypeptide gene of *Autographa californica* nuclear polyhedrosis virus. Virology **139:**414–418.
25. **Langridge, W. H. R.** 1983. Virus DNA replication and protein synthesis in *Amsacta moorei* entomopoxvirus-infected *Estigmene acrea* cells. J. Invertebr. Pathol. **41:**341–349.
26. **Langridge, W. H. R., and D. W. Roberts.** 1982. Structural proteins of *Amsacta moorei*, *Euxoa auxilaris*, and *Melanopus sanguinipes* entomopoxviruses. J. Invertebr. Pathol. **39:**346–353.
27. **Lin, K., and S. Y. Cheng.** 1991. An efficient method to purify active eukaryotic proteins from the inclusion bodies of *Escherichia coli*. BioTechniques **11:**748–751.
28. **Luftig, R. B.** 1982. Does the cytoskeleton play a significant role in animal virus replication? J. Theor. Biol. **99:**173–191.
29. **Lytvyn, V., Y. Fortin, M. Banville, B. Arif, and C. Richardson.** 1992. Comparison of the thymidine kinase genes from three entomopoxviruses. J. Gen. Virol. **73:**3235–3240.
30. **Marlow, S., L. J. Billam, C. P. Palmer, and L. A. King.** 1993. Replication and morphogenesis of *Amsacta moorei* entomopoxvirus in cultures cells of *Estigmene acrea* (salt marsh caterpillar). J. Gen. Virol. **74:**1457–1461.
31. **Marlow, S. J., C. P. Palmer, and L. A. King.** 1992. Cytopatic effects of *Amsacta moorei* entomopoxvirus infection on the cytoskeleton of *Estigmene acrea* cells. Virus Res. **26:**41–55.
32. **Matsudaira, P.** 1987. Sequence from picomole quantities of proteins electroblotted onto polyvinylene difluoride membranes. J. Biol. Chem. **262:** 10035–10038.
33. **Matthews, R. E. F.** 1982. Classification and nomenclature of viruses. Fourth report of the International Committee on Taxonomy of Viruses. Intervirology **17:**4–199.
34. **Moss, B.** 1990. Poxviridae and their replication, p. 2079–2111. *In* B. N. Fields (ed.), Virology, 2nd ed. Raven Press, New York.
35. **Moss, B., B.-Y. Ahn, B. Amegadizie, P. D. Gershon, and J. G. Keck.** 1991. Cytoplasmic transcription system encoded by vaccinia virus. J. Biol. Chem. **266:**1355–1358.
36. **Nilsson, B., L. Abrahmsen, and M. Uhlen.** 1985. Immobilization and purification of enzymes with staphylococcal protein A gene fusion vectors. EMBO J. **4:**1075–1080.
37. **Nilsson, B., G. Forsberg, and M. Hartmanis.** 1991. Expression and purification of recombinant insulin-like growth factors from *Escherichia coli*. Methods Enzymol. **198:**3–16.
38. **Palmer, C. P., D. P. Miller, S. A. Marlow, L. E. Wilson, L. M. Lawrie, and L. A. King.** 1995. Genetic modification of an entomopoxvirus: deletion of the spheroidin gene does not affect virus replication *in vitro*. J. Gen. Virol. **76:**15–23.
39. **Penman, S.** 1985. Virus metabolism and cellular architecture, p. 169–182. *In* B. N. Fields (ed.), Virology, 1st ed. Raven Press, New York.
40. **Postle, K., and R. F. Good.** 1983. DNA sequence of the *Escherichia coli* tonB gene. Proc. Natl. Acad. Sci. USA **80:**5235–5239.
41. **Rice, S. A., M. C. Long, V. Lam, and C. A. Spencer.** 1994. RNA polymerase II is aberrantly phosphorylated and localized to viral replication compartments following herpes simplex virus infection. J. Virol. **68:**988–1001.
42. **Richardson, J. P., R. P. Beecroft, D. L. Tolson, M. K. Liu, and T. W. Pearson.** 1988. Procyclin: an unusual immunodominant glycoprotein surface antigen from the procyclic stage of African trypanosomes. Mol. Biochem. Parasitol. **31:**203–216.
43. **Roberts, S., I. Ashmole, L. J. Gibson, S. M. Rookes, G. J. Barton, and P. H. Gallimore.** 1994. Mutational analysis of human papillomavirus E4 proteins: identification of structural features important in the formation of cytoplasmic E4/cytokeratin networks in epithelial cells. J. Virol. **68:**6432–6445.
44. **Stokes, G. V.** 1976. High-voltage electron microscope study of the release of vaccinia virus from whole cells. J. Virol. **18:**636–642.
45. **Summers, M. D., and G. E. Smith.** 1987. A manual of methods for baculovirus vectors and insect cell culture procedures. Bulletin 1555. Texas Agricultural Experiment Station and Texas A&M University, College Station, Tex.
46. **Traub, I., S. Gaisser, and V. Braun.** 1993. Activity domains of the TonB protein. Mol. Microbiol. **2:**409–423.
47. **Van der Wilk, F., J. W. M. Van Lent, and J. M. Vlak.** 1987. Immunogold detection of polyhedrin, p10, and virion antigens in *Autographa californica* nuclear polyhedrosis virus-infected *Spodoptera frugiperda* cells. J. Virol. **68:** 2615–2623.
48. **Van Oers, M. M., J. T. Flipsen, C. B. Reusken, E. L. Sliwinsky, R. W. Goldbach, and J. M. Vlak.** 1993. Functional domains of the p10 protein of *Autographa californica* nuclear polyhedrosis virus. J. Gen. Virol. **74:**563–574.
49. **Van Oers, M. M., J. T. M. Flipsen, C. B. F. M. Reusken, and J. M. Vlak.** 1994. Specificity of baculovirus p10 functions. Virology **200:**513–523.
50. **Van Ormondt, H., J. Maat, and C. P. van Beveren.** 1980. The nucleotide sequence of the transforming early region of adenovirus type 5 DNA. Gene **11:**299–309.
51. **Vialard, J. E., and C. D. Richardson.** 1993. The 1,629-nucleotide open reading frame located downstream of the *Autographa californica* nuclear polyhedrosis virus polyhedrin gene encodes a nucleocapsid-associated phosphoprotein. J. Virol. **67:**5859–5866.
52. **Vlak, J. M., F. A. Klinkenberg, K. J. M. Zaal, M. Usmany, E. C. Klinge-Roode, J. B. F. Geervliet, J. Roosien, and J. W. M. van Lent.** 1988. Functional studies on the p10 gene of *Autographa californica* nuclear polyhedrosis virus using a recombinant expressing a p10-β-galactosidase fusion gene. J. Gen. Virol. **69:**765–776.
53. **Volkman, L. E., P. A. Goldsmith, and R. T. Hess.** 1987. Evidence for filament involvement in budded *Autographa californica* nuclear polyhedrosis virus production. Virology **156:**32–39.
54. **Weyer, U., S. Knight, and R. D. Possee.** 1990. Analysis of very late gene expression by *Autographa californica* nuclear polyhedrosis virus and the further development of multiple expression vectors. J. Gen. Virol. **71:**1525–1534.
55. **Williams, G. V., D. Z. Rohel, J. Kuzio, and P. Faulkner.** 1989. A cytopathological investigation of *Autographa californica* nuclear polyhedrosis virus p10 gene function using insertion/deletion mutants. J. Gen. Virol. **70:**187–202.
56. **Williamson, M. P.** 1994. The structure and function of proline-rich regions in proteins. Biochem. J. **297:**249–260.
57. **Zorzato, F., J. Fujii, K. Otsu, M. Phillips, N. M. Green, F. A. Lai, G. Meissner, and D. H. MacLennan.** 1990. Molecular cloning of cDNA encoding human and rabbit forms of the Ca^{+2} release channel ryanodine receptor of skeletal muscle sarcoplasmic reticulum. J. Biol. Chem. **265:**2244–2256.

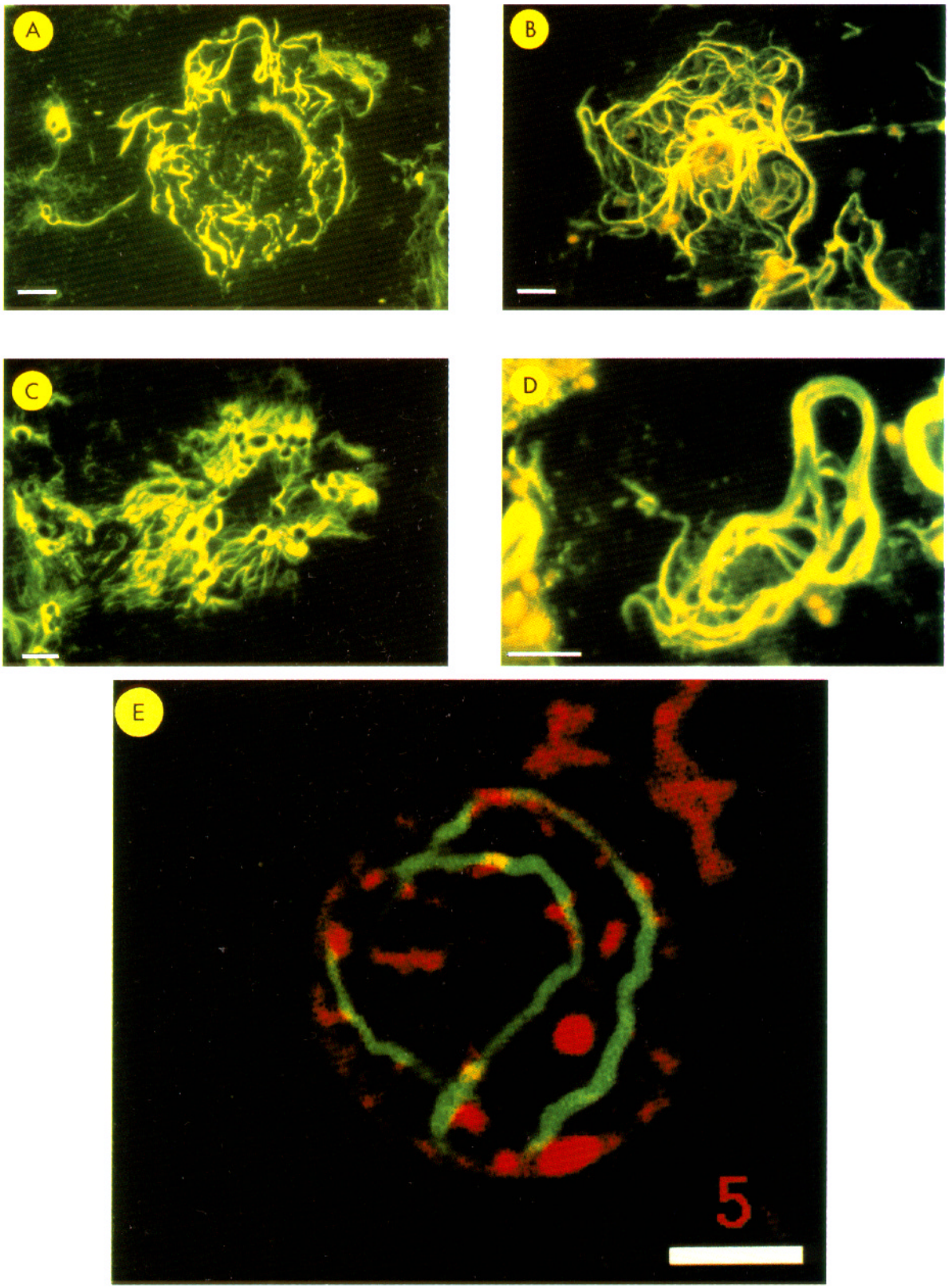
A
B
C
D
E
5